

Infant and Adult Inhalation Exposure to Resuspended Biological Particulate Matter

Tianren Wu,^{†,‡} Martin Täubel,[§] Rauno Holopainen,^{||} Anna-Kaisa Viitanen,[⊥] Sinikka Vainiotalo,[⊥] Timo Tuomi,[⊥] Jorma Keskinen,[#] Anne Hyvärinen,[§] Kaarle Hämeri,[▽] Sampo E. Saari,[#] and Brandon E. Boor^{*,†,‡,Ⓞ}

[†]Lyles School of Civil Engineering, Purdue University, 550 Stadium Mall Drive, West Lafayette, Indiana 47907, United States

[‡]Ray W. Herrick Laboratories, Center for High Performance Buildings, Purdue University, 177 South Russell Street, West Lafayette, Indiana 47907, United States

[§]National Institute for Health and Welfare, P.O. Box 95, Kuopio, FI 70701, Finland

^{||}Oulu University of Applied Sciences, P.O. Box 222, Oulu, FI 90101, Finland

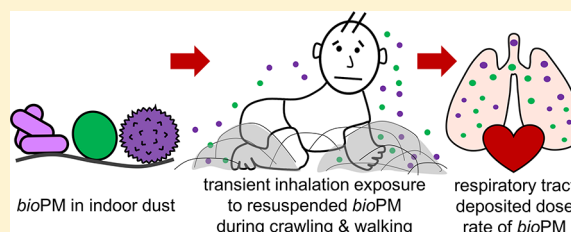
[⊥]Finnish Institute of Occupational Health, P.O. Box 40, Helsinki, FI 00250, Finland

[#]Department of Physics, Tampere University of Technology, P.O. Box 692, Tampere, FI 33101, Finland

[▽]Department of Physics, University of Helsinki, P.O. Box 64, Helsinki, FI 00014, Finland

Supporting Information

ABSTRACT: Human-induced resuspension of floor dust is a dynamic process that can serve as a major indoor source of biological particulate matter (*bioPM*). Inhalation exposure to the microbial and allergenic content of indoor dust is associated with adverse and protective health effects. This study evaluates infant and adult inhalation exposures and respiratory tract deposited dose rates of resuspended *bioPM* from carpets. Chamber experiments were conducted with a robotic crawling infant and an adult performing a walking sequence. Breathing zone (BZ) size distributions of resuspended fluorescent biological aerosol particles (FBAPs), a *bioPM* proxy, were monitored in real-time. FBAP exposures were highly transient during periods of locomotion. Both crawling and walking delivered a significant number of resuspended FBAPs to the BZ, with concentrations ranging from 0.5 to 2 cm⁻³ (mass range: ~50 to 600 μg/m³). Infants and adults are primarily exposed to a unimodal FBAP size distribution between 2 and 6 μm, with infants receiving greater exposures to super-10 μm FBAPs. In just 1 min of crawling or walking, 10³–10⁴ resuspended FBAPs can deposit in the respiratory tract, with an infant receiving much of their respiratory tract deposited dose in their lower airways. Per kg body mass, an infant will receive a nearly four times greater respiratory tract deposited dose of resuspended FBAPs compared to an adult.



INTRODUCTION

House dust is enriched with microorganisms and allergen-carrying particles of indoor and outdoor origin (see literature review in [section S1](#); note: section, table, and figure numbers preceded by an “S” are in the [Supporting Information \(SI\)](#)). Release of this dust into the air due to human movement-induced resuspension may represent a significant pathway by which we are exposed to microbes and allergens. Resuspension is a major indoor source of coarse-mode (>1 μm) abiotic and biological particulate matter (or *bioPM*), such as bacterial cells and fungal spores.^{1–6} Simply walking across a carpet can release on the order of 10 to 100 million particles per minute.⁷ Inhalation exposure to the microbial and allergenic content of indoor dust is associated with both protective and adverse health effects in humans and may play a key role in shaping the lung microbiome ([section S1](#)). Despite the health and environmental significance of indoor dust, which is widely used as a long-term inhalation exposure surrogate, we have a

limited understanding of the relationship between particle resuspension induced by age-dependent forms of locomotion, such as crawling and walking, with the transient exposures and respiratory tract deposited doses of *bioPM* that are received by infants, children, and adults.

Resuspension is influenced by different forms of physical activity.^{7,8} Evolution of human locomotion during the first year of life involves an array of complex near-floor movements that transition toward various forms of crawling at around 6 months and eventually to walking between 12 and 14 months.⁹ Very little is known as to how the crawling motion of an infant resuspends indoor dust and the resulting size distributions of

Received: August 14, 2017

Revised: November 11, 2017

Accepted: November 16, 2017

Published: November 16, 2017

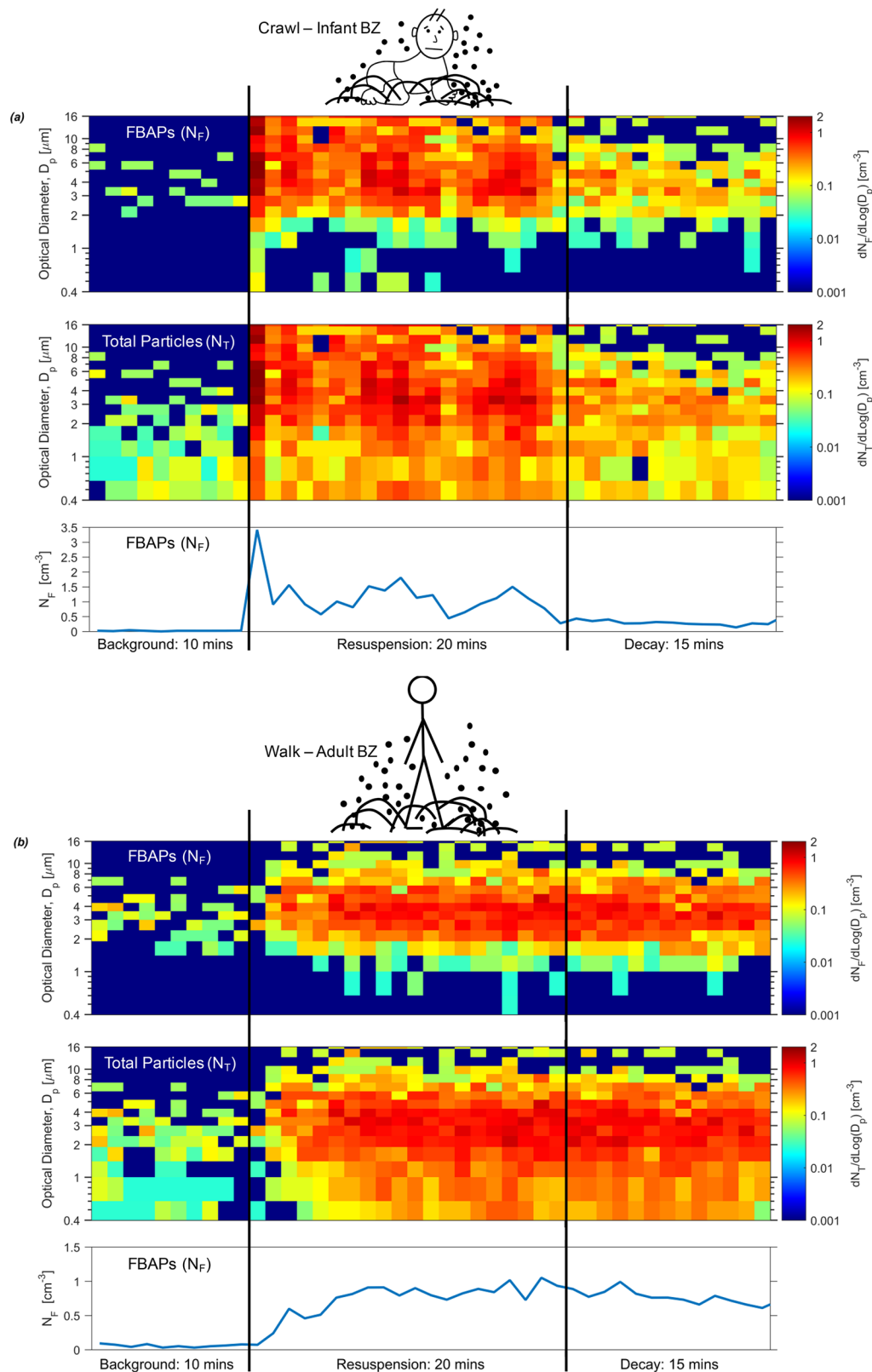


Figure 1. Time-series plots of FBAP number size distributions ($dN_F/d\log D_p$, upper), total particle number size distributions ($dN_T/d\log D_p$, middle), and size-integrated ($0.4\text{--}15.4\ \mu\text{m}$) FBAP number concentrations (N_F , lower) for (a) an infant crawling resuspension experiment and (b) adult walking resuspension experiment on carpet 3.

resuspended *bioPM* an infant is exposed to in their near-floor microenvironment.^{10–12}

Recent advances in DNA-based methods and laser-induced fluorescence (LIF) techniques for *bioPM* identification and

quantification allow for improved *bioPM* exposure assessment beyond what can be achieved with traditional culture-based methods.¹³ LIF-based aerosol instrumentation can be used to study the transport of resuspended *bioPM* to the infant and

adult breathing zone (BZ) at the short time-scales of relevance to resuspension (e.g., seconds to minutes) and at high size-resolution. LIF techniques target the intrinsic biological fluorophores of bacterial cells, fungal spores, and pollen grains, such as amino acids (e.g., tryptophan, phenylalanine, and tyrosine), flavins, and coenzymes (e.g., nicotinamide adenine dinucleotide (NADH)).^{14–16} LIF can reliably detect and discriminate supermicron *bio*PM from abiotic particles and is generally viewed as a lower limit of total *bio*PM, or primary biological aerosol particles (PBAPs), as some *bio*PM exhibit little to no fluorescence.^{16,17} Abiotic particles can fluoresce; however, nonbiological interference is generally of concern for submicron particles,^{16,18} as discussed in detail in Table S3. Particles whose fluorescence properties are within the excitation–emission operational range of a LIF-based instrument are registered as fluorescent biological aerosol particles, or FBAPs (Table S2). When integrated in tandem with quantitative PCR (qPCR) and next-generation sequencing (NGS), LIF is a valuable tool to advance knowledge on exposures to *bio*PM released from inherently episodic indoor emission sources, such as resuspension.

Inhalation exposure to resuspended *bio*PM can be better linked to cellular response in the lungs and respiratory and allergic health outcomes in infants and adults through size-resolved respiratory tract deposited dose rate (RTDDR) analysis.¹⁹ The number, surface area, and mass of particles deposited in each region of the respiratory system per unit time are determined through integration of respiratory tract deposition fractions and BZ particle size distributions. Few studies have reported RTDDRs,^{20–27} and it has yet to be used for *bio*PM measurements made in situ in the infant and adult BZ or for assessing exposure to indoor dust. This is in part due to the difficulty of measuring BZ particle size distributions with heavy aerosol instrumentation, especially for infants and young children. More broadly, empirically based doses and uptake rates for environmental stressors as determined for infant-specific physiologies, in this case, the respiratory system and crawling posture, are needed to elucidate the key factors affecting health during the most critical stages of human development.²⁸

The primary aim of this study is to mechanistically link infant crawling-induced and adult walking-induced resuspension of carpet dust with transient *bio*PM exposure and regional respiratory tract deposited dose rate analysis via application of real-time (1 Hz) LIF monitoring of FBAPs in the infant and adult BZ in controlled chamber experiments. This study makes unique use of a custom-built simplified mechanical crawling infant to measure resuspended FBAP size distributions in the infant BZ during crawling. Here, FBAPs are viewed as a proxy for total *bio*PM, supplemented with off-line qPCR and NGS analysis.

MATERIALS AND METHODS

Experimental Design. Resuspension experiments were conducted in an environmentally controlled chamber with a volume of 81.4 m³ operating at an air exchange rate of 0.66 h⁻¹ (Figures S2–S4). Five carpets borrowed from residents in Helsinki, Finland were used in the resuspension experiments and tested as-is (Table S1 and Figure S1). Five crawling and five walking resuspension experiments, each 45 min in duration, were conducted along different linear paths on each carpet, for a total of 50 individual experiments. Each resuspension experiment consisted of three periods: (1) a 10 min

background period in which the chamber was vacant, (2) a 20 min crawling- or walking-induced resuspension period, and (3) a 15 min decay period in which the chamber was vacant (Figure 1). A simplified mechanical crawling infant performing a modified belly crawl was used to simulate the crawling locomotion of an infant in a repeatable manner, as described in section S2 (see the SI video). The walking experiments were conducted by an adult volunteer wearing a full clean suit outfit with booties and a hood, nitrile gloves, and a filter mask. Additional details on the chamber operating conditions, resuspension sequences, and quality control measures are included in section S2.

Aerosol Instrumentation. FBAP (N_F) and total (sum of fluorescent and nonfluorescent particles; N_T) particle number size distributions from 0.4 and 15.4 μm were monitored throughout each resuspension sequence with a LIF-based aerosol instrument, the BioScout (ENVI BioScout, EnviroNics Ltd., Mikkeli, Finland). Details on the operational principle of the BioScout are provided in Table S2 and in Saari et al.^{17,29,30} Total particle number size distributions from 0.314 to 11.2 μm were also monitored with an optical particle sizer (OPS, model 3330, TSI Inc., Shoreview, MN, U.S.A.). In the following sections of the paper, all references to measured particle size or diameter are based on the optical diameters reported by both instruments. Gravimetric and DNA-based analysis of the resuspended particles and settled carpet dust was also performed, as described in section S2 and our parallel study Hyytiäinen et al.³¹ For the crawling experiments, the BioScout and OPS were placed on a mobile trolley that followed in parallel to the robot, with sampling inlets at the approximate breathing zone (BZ) height of an infant performing a belly crawl (25 cm).³² For the walking experiments, the instruments were placed on a stand in the middle of the carpet, with the sampling inlets at the adult BZ height (150 cm).

Analysis of Respiratory Tract Deposited Dose Rates of Resuspended *bio*PM (FBAPs). The size distributions of resuspended FBAPs (*bio*PM proxy) measured in the infant and adult BZs were used to estimate total, regional, and weight-normalized FBAP RTDDRs (RTDDR_F, no. or μm^2 of FBAPs deposited per minute of crawling or walking) for a defined set of age-specific breathing conditions and hygroscopic growth parameters (section S2). Size-resolved deposition fractions were obtained by using the age-specific symmetric single-path model from the open-source Multiple-Path Particle Dosimetry (MPPD) Model (v3.04, Applied Research Associates, Inc., Albuquerque, NM, U.S.A.; Figure S6). Walking-induced size-resolved FBAP emission rates (E_F , no. of FBAPs emitted per hour) were also estimated (section S2 and Figure S2).

RESULTS AND DISCUSSION

A detailed summary of the 50 resuspension experiments is presented in Table S4, including FBAP and total particle number and mass concentrations and modal log-normal fitting parameters of mean FBAP and total particle number size distributions. Supplemental results, statistical analysis, and study limitations are presented in section S3, including size-resolved emission rates of FBAPs during walking, discussion on *bio*PM resuspension mechanisms, and comparisons between LIF and qPCR for indoor microbial exposure assessments.

Crawling and Walking Resuspension Sequence and Transient Exposure to Resuspended *bio*PM (FBAPs). Figure 1 illustrates the transient nature, on a time scale on the order of 1 min, of human movement-induced resuspension of

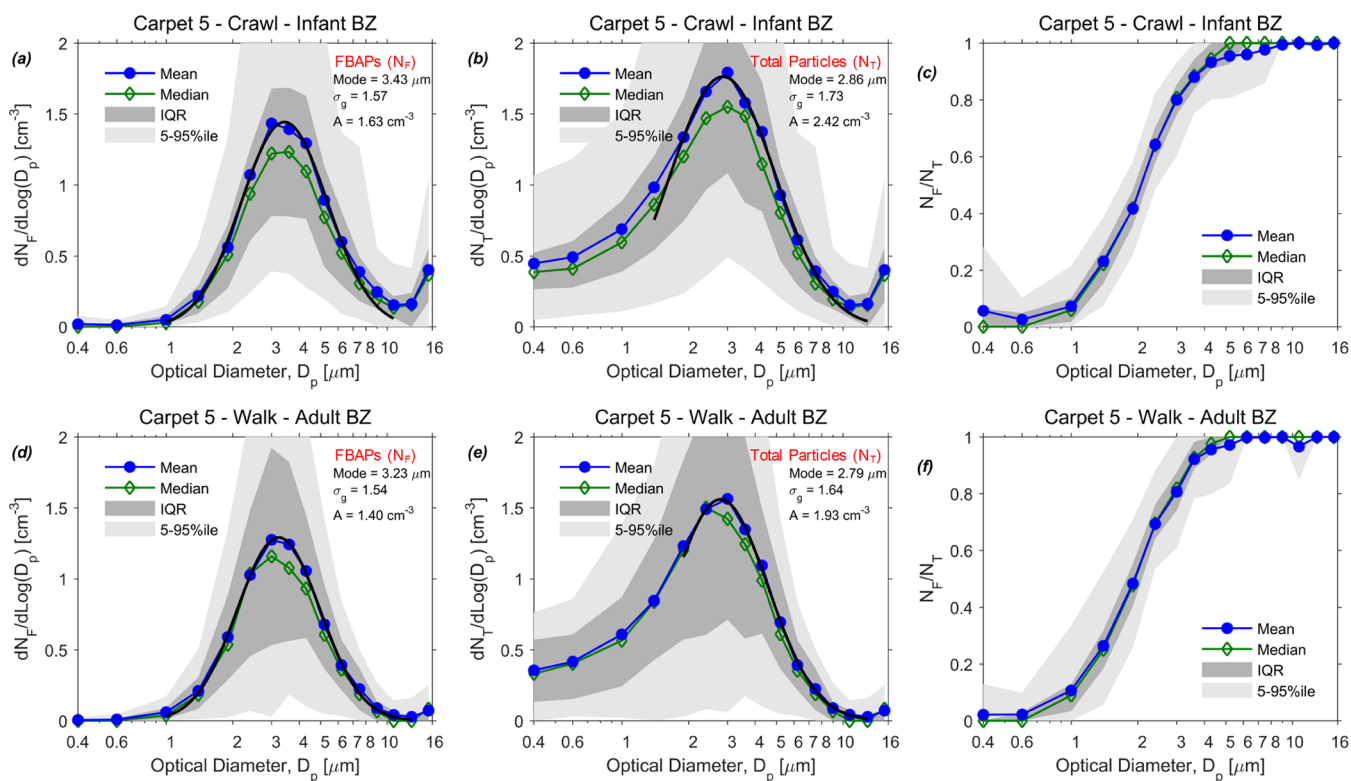


Figure 2. Carpet-averaged $dN_F/d\log D_p$ (left), $dN_T/d\log D_p$ (middle), and size-resolved N_F/N_T ratios (right) measured during the crawling (a–c) and walking (d and e) periods on carpet 5. Blue curves represent mean values, green curves represent median values, dark gray regions represent the interquartile range (IQR), and light gray regions represent the 5–95th percentile range among five crawling or walking paths on the same carpet (100 min in total). Black curves show the log-normal fitting of the dominant peaks. The mode, geometric standard deviation (σ_g), and amplitude (A) are presented.

FBAPs from carpet dust and the infant and adult inhalation exposures that occur both during and after a resuspension event. The characteristic time-series plots of FBAP and total particle number size distributions and size-integrated (0.4–15.4 μm) FBAP number concentrations that are shown in Figure 1 for crawling and walking on carpet 3 are representative of what was observed across all 50 resuspension experiments (Figure S8). The temporal dynamics of *bioPM* resuspension due to the crawling motion of an infant are presented in this paper for the first time, to the authors' knowledge, enabled by the high sampling rate of a LIF-based aerosol instrument.

There are distinct differences in the time-evolution of resuspended FBAP concentrations between crawling and walking. For infants, an abrupt burst of resuspended FBAPs in the infant BZ can be observed at the onset of crawling (Figure 1a), after which the FBAP concentration fluctuated with respect to time during the remainder of the resuspension period and decreased rapidly during the decay period. The initial, short-term peak in FBAPs in the air around the infant was observed in nearly every resuspension experiment, with concentrations often in the range of 2–4 cm^{-3} , far exceeding concentrations of FBAPs in the adult BZ during walking. The accelerated decay in FBAP concentrations postcrawling suggests that an infant will receive much of their exposure to self-induced resuspended *bioPM* during periods where they are actively engaged in movement. This was found to be especially true for FBAPs larger than 7 μm in size. Given the idiosyncratic behavior patterns and movements of infants during their first year of life,⁹ one would expect the concentrations of *bioPM* in the infant BZ to vary from minute to minute, as the child

crawls, stops to sit and play with toys, and then continues crawling.

An adult walking across a carpet will be exposed to a gradual rise in concentrations of resuspended *bioPM* throughout the duration of their movement (Figure 1b). After 10–15 min of walking, FBAP concentrations approach a near steady-state condition, followed by a slow decay as activity ceases. The enhanced mixing of the chamber air associated with the walking motion of an adult aids in the dispersion of FBAPs, prolonging exposure to biological material in floor dust well beyond the duration of the resuspension event itself.

The sporadic and time variant nature of crawling-induced FBAP resuspension appears to be distinctly unique to a crawling infant. Incomplete mixing of air around the infant may be one of the drivers for this phenomenon, along with the high deposition rates for the coarse-mode particles (Figure S5), random contact locations of the small stomping hands of the robotic platform, and spatial variability in the dust deposits along the crawling path. The latter two may give rise to periods of high and low FBAP concentrations during the resuspension period, depending on the magnitude of the surface loading of the settled particles that are agitated at each point of contact.

Resuspended FBAP Number and Mass Size Distributions and Concentrations in the Infant and Adult Breathing Zones. Size distributions of resuspended FBAPs in the infant and adult BZs displayed a unimodal log-normal distribution, exhibiting a prominent mode between 3 and 5 μm , while a partial second mode was observed for super-10 μm FBAPs in the infant BZ (Figure 2). This is illustrated in Figure 2 for the crawling and walking resuspension experiments on

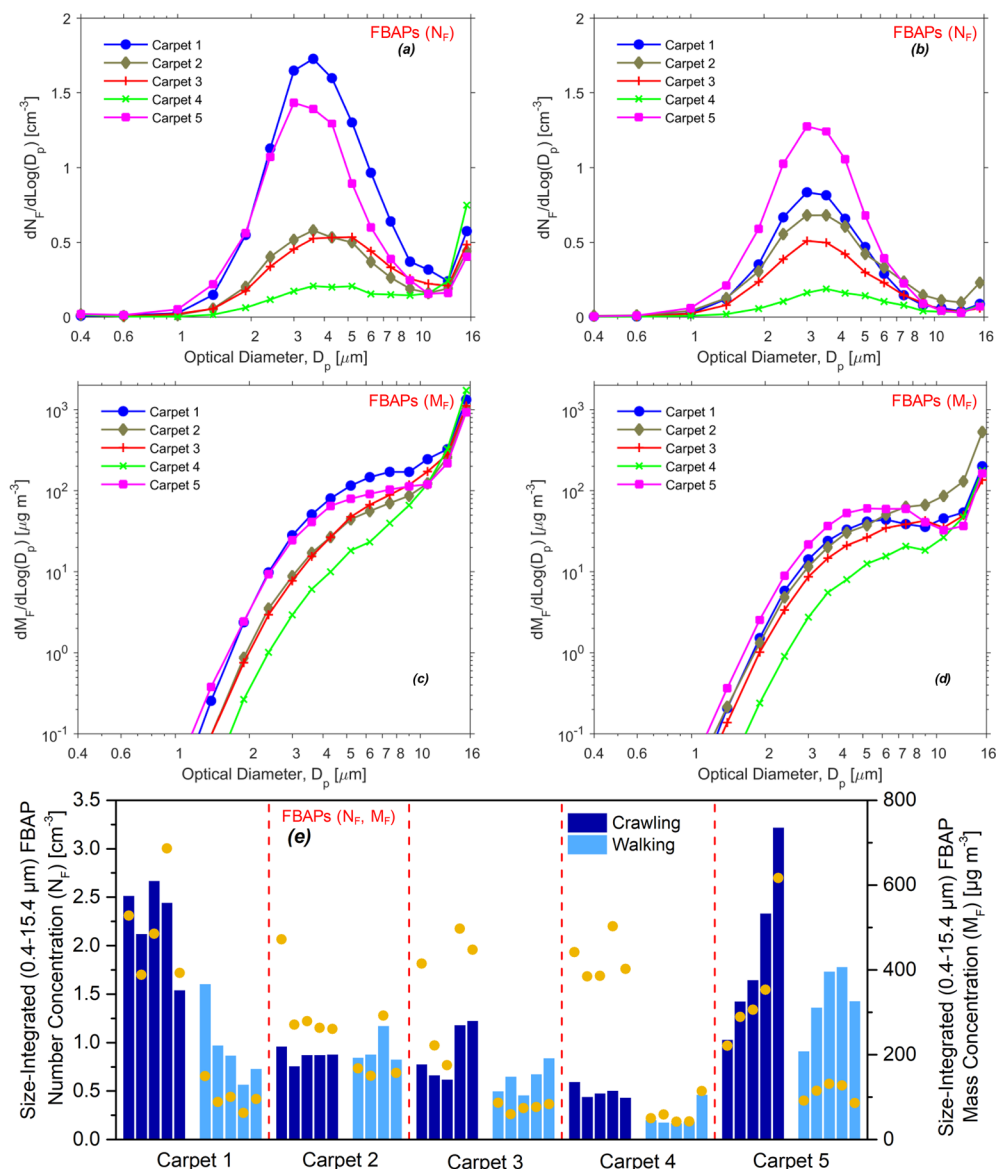


Figure 3. Carpet-averaged mean FBAP number ($dN_F/d\log D_p$) and mass ($dM_F/d\log D_p$) size distributions measured during resuspension periods on five carpets for both crawling (a and c) and walking (b and d) experiments; (e) mean size-integrated (0.4–15.4 μm) FBAP number concentrations (N_F , blue bars) and size-integrated (0.4–15.4 μm) FBAP mass concentrations (M_F , yellow dots) measured in each sequential path on each carpet during the resuspension periods. Note: when computing M_F , FBAPs are assumed to be spherical with a ρ of 1.204 g cm^{-3} from the OPS calibration (section S2) and particles below $\sim 1 \mu\text{m}$ are not shown in the $dM_F/d\log D_p$ plots to improve visibility of the partial super-10 μm mode.

carpet 5. Size distributions for the remaining carpets are provided in Figure S9. Modal diameters of the FBAP size distributions among the five carpets ranged from 3.43 to 4.42 μm for the infant BZ and from 3.23 to 3.78 μm for the adult BZ. The total particle size distributions (Figure 2b,e) displayed a broader mode with modal diameters that were generally 0.5–1 μm smaller than those of the FBAP distributions. The geometric standard deviations of the dominant 3–5 μm FBAP mode varied from 1.54 to 1.80, indicating that the mode is associated with different types of *bio*PM.¹⁴ While the focus of this paper is on *bio*PM, the results and analysis for total particle size distributions are useful in evaluating human inhalation exposure to chemical contaminants in indoor dust, such as particle-bound semivolatile organic compounds (SVOCs).

Most of the coarse-mode resuspended particles were fluorescent. Figure 2c,f shows the size-resolved ratios of FBAPs to total particles (N_F/N_T). Above 1 μm , N_F/N_T

increased sharply with size, reaching approximately 0.8 for 3 μm particles and nearly unity for particles larger than 8 μm . Very few of the sub-1 μm particles fluoresced. The high N_F/N_T ratios for particles larger than 1 μm in size suggest that a significant fraction of the resuspended coarse mode particles is comprised of *bio*PM; abiotic particles with surface adhered biological material, such as clusters of skin fragments (squames) and skin-associated bacteria; and nonmicrobial fluorescent interferents (Table S3). It is also possible that some of the high intensity scattered light from these large particles leaked to the fluorescence detector, causing a positive artifact to fluorescent particle detection. The N_F/N_T trend presented here is consistent with a previous indoor FBAP study³³ but greater than those reported in outdoor FBAP measurements.^{14,34,35}

The results of the qPCR analysis and bacterial 16S rRNA gene sequencing of the resuspended particles collected with filter samplers offer some clues on the origin of the highly

fluorescent resuspended particles in the dominate 3 and 5 μm mode (section S2³¹). The most abundant identified bacterial phyla and genera included: Proteobacteria (50–55% (percentage of relative abundance), genera: *Oxalobacteraceae gen., Acinetobacter, Paracoccus*); Actinobacteria (20–25%, genera: *Corynebacterium, Micrococcus, Propionibacterium*); Firmicutes (~15%, genera: *Staphylococcus, Streptococcus, Clostridium*); and Bacteroidetes (<10%, genera: *Sediminibacterium*). Quantified fungal groups included: *Penicillium spp., Aspergillus spp., Paecilomyces variotii,* and *Cladosporium herbarum*. The concentration of bacterial cell equivalents (CEs) in both the carpet dust and infant and adult BZ were more than 1 order of magnitude greater than that for fungal CEs. Thus, bacteria likely contribute much more to the resuspended FBAP concentrations reported here than do fungi.

Single cells of many bacterial species are approximately 1 μm or smaller in size,³⁶ including species of genera identified in this study: *Micrococcus luteus* (equivalent optical diameter (EOD): 0.9 μm), *Staphylococcus aureus* (EOD: 0.7 μm), and *Acinetobacter baumannii* (EOD: 1.1 μm).³⁷ However, very few resuspended FBAPs 1 μm or smaller were observed in the infant and adult BZ. As documented in numerous studies, this finding suggests that the bacterial cells preferentially exist in the form of cellular agglomerates larger than 2 μm or carried on larger nonmicrobial particles.^{14,33,36,38–44} Spores of the four quantified fungal groups are typically 2–4 μm in both EOD and aerodynamic diameter.^{20,37,45–47} Thus, the dominant 3 to 5 μm FBAP mode was likely comprised of bacterial cell agglomerates and, to a lesser extent, fungal spores. However, sub-10 μm fluorescing mite and animal allergen-carrying particles, squames, and pollen grains may also contribute to this mode.^{37,48–50}

FBAP number concentrations were greater in the infant BZ during crawling compared to the adult BZ during walking for four out of five carpets,^{1,3–5} with infant BZ FBAP mass concentrations (M_F) greater than those in the adult BZ for all five carpets (Figure 3e). For carpets 1 and 4, an infant's exposure to resuspended FBAPs was 2.4-fold and 2-fold greater than that of an adult, respectively (number basis). The average size-integrated number concentration of FBAPs from 0.4 to 15.4 μm across all crawling paths on the five carpets was $1.285 \pm 0.794 \text{ cm}^{-3}$ (mean \pm s.d.) and $0.830 \pm 0.470 \text{ cm}^{-3}$ for the walking paths (Table S4). This results in average inhalation intakes ($N_F \times$ breathing rate) of 7.68×10^3 and 1.62×10^4 inhaled FBAPs per minute for infants and adults, respectively (breathing rates in section S2). To put these values in perspective, the daily average FBAP number concentration reported for an occupied classroom was 0.039 cm^{-3} (UV-APS³³) and the average FBAP concentrations in an adult's and children's hospital were 0.06 and 0.03 cm^{-3} , respectively (UV-APS⁵¹). It is important to note that these two studies were not aimed at FBAP exposure assessment, sampled in the bulk room air, and account for a wide variation in occupancy and activity patterns. Intermittent and short-term exposures to elevated concentrations of FBAPs, on the order of 1 cm^{-3} , during active periods of locomotion, as evaluated in this study (Figures 1 and 3), may contribute significantly to the daily cumulative FBAP exposures of infants and adults. However, personal exposures to resuspended bioPM at the high time resolution afforded by LIF have yet to be measured in field conditions.

The inhalation height of a crawling infant (25 cm) was associated with greater numbers of FBAPs larger than 3 μm compared to that of an adult (1.5 m; Figures 1, 2, S8, and S9).

This trend can be observed by noticing that the geometric mean diameter of the dominant FBAP mode was larger during crawling than while walking, ranging from a fraction of a micrometer for carpet 5 to as much as 1.03 μm for carpet 3. The fraction of size-integrated FBAP number concentrations (0.4–15.4 μm) attributed to particles in the size range of 7.5 to 15.4 μm were (from carpets 1 to 5): 0.12, 0.20, 0.23, 0.47, and 0.10 for the crawling experiments and 0.05, 0.11, 0.07, 0.14, and 0.03 for the walking experiments. Furthermore, the development of a second, larger mode in the 10–15.4 μm range was identified in the infant BZ. This partial mode was particularly strong for carpets 2–4 and dominates the FBAP mass size distributions (Figure 3c,d). While this mode could not be fully captured given the upper size-limit of the BioScout, it suggests that infants will be exposed to a greater number of super-10 μm resuspended bioPM compared to adults. bioPM in this size range include multicellular fungal spores, pollen grains, and abiotic bioPM carrier particles.^{36,43} Fluorescing squames and clothing fabric fibers may also contribute to the observed super-10 μm FBAPs (Table S3).

Crawling- and walking-induced resuspension contributed minimally to concentrations of sub-1 μm FBAPs in the BZ ($N_F < 0.01 \text{ cm}^{-3}$) but were associated with a meaningful elevation of nonfluorescent sub-1 μm particles, especially for carpets 1 and 2 (Figures 1, 2, S8, and S9). This suggests that sub-1 μm bioPM, such as some single bacterial cells, fungal fragments, and subpollen particles,^{52,53} are either preferentially carried on larger particles or in an agglomerated state, are very weakly fluorescent, or are sparsely present in the dust deposits of the five carpets. The former two are most likely, given the tendency of bioPM to exist as agglomerates and previous reports of weakly fluorescent bioPM in the 0.5–1 μm range.⁴² The resuspension of sub-1 μm nonfluorescent particles as small as 0.4 μm is consistent with previous resuspension studies on adult footfalls.⁵⁴

Infant and adult exposure to resuspended FBAPs is influenced by the carpet and dust deposit over which the activity is occurring (Figure 3). Carpet-to-carpet variability is shown in Figure 3 for FBAP number and mass size distributions and concentrations. Although the shape of the FBAP size distributions were similar, their lognormally fitted modal number concentrations spanned nearly 1 order of magnitude, from 0.29 cm^{-3} for crawling on carpet 4 to 2.11 cm^{-3} for crawling on carpet 1. The highest FBAP number concentrations occurred for crawling and walking on carpets 1 and 5 (Figure 3e), with N_F exceeding 1 cm^{-3} for most of the resuspension events. Wool carpets from the same Helsinki residence (carpet 1 from the bedroom and carpet 3 from the corridor, two occupants, one indoor cat named Gustave) exhibited markedly different FBAP size distributions during crawling, with the lognormally fitted modal amplitude of carpet 1 (2.11 cm^{-3}) 2.6-fold greater than that of carpet 3 (0.80 cm^{-3} ; Figures 3 and S9). BZ FBAP mass concentrations (0.4–15.4 μm) varied among the five carpets (Figure 3e) and were typically in the range of 50–600 $\mu\text{g}/\text{m}^3$, exceeding 600 $\mu\text{g}/\text{m}^3$ for one crawling path on carpets 1 and 5. Despite differences in FBAP size distributions, the size-resolved N_F/N_T ratio curves were similar among all five carpets and for both crawling and walking (Figure S10).

The five carpets exhibited variations in dust mass loading (2.63–16.72 g/m^2), total particle number concentrations in the settled dust ($\sim 10^9$ to 10^{10} no./ m^2), and bacterial and fungal cell concentrations in the settled dust (Table S1 and Figure S7). While crawling on carpets 2 and 3 contributed similar levels of

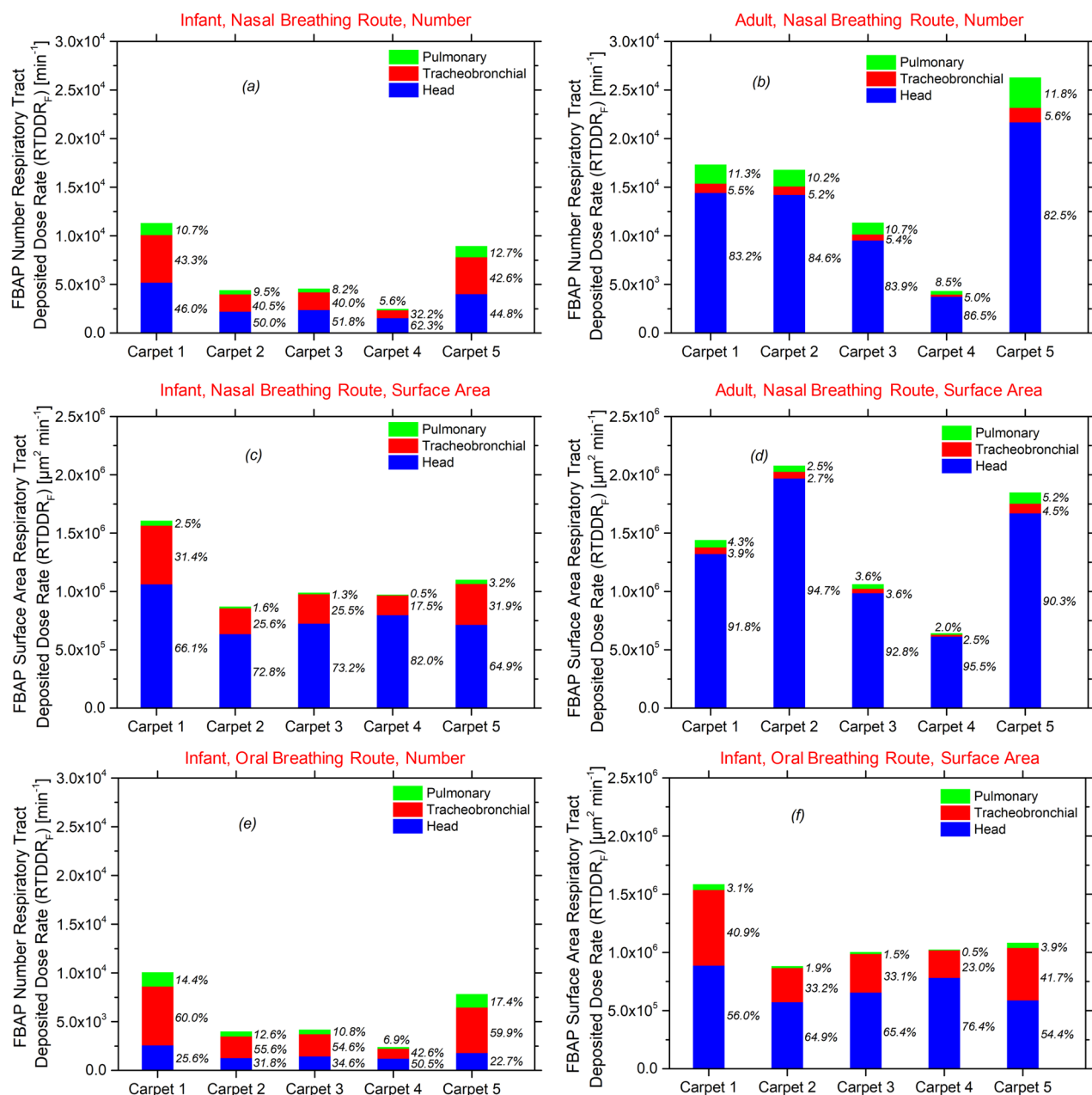


Figure 4. Total and regional size-integrated ($0.4\text{--}15.4\ \mu\text{m}$) FBAP respiratory tract deposited dose rates (RTDDR_Fs; per minute crawling or walking) for each of the five carpets: (a) infant, nasal breathing route, number, (b) adult, nasal breathing route, number, (c) infant, nasal breathing route, surface area, (d) adult, nasal breathing route, surface area, (e) infant, oral breathing route, number, and (f) infant, oral breathing route, surface area. The fractional dose in each region, expressed as a percentage, is shown to the right of each bar. Note: a hygroscopic growth factor of 1.12 was applied to the BZ FBAP size distributions, as described in section S2.

FBAPs to the infant BZ, 0.866 and $0.890\ \text{cm}^{-3}$, respectively, carpet 2 had a dust load 3.17-fold greater than carpet 3 with 3.44 times as many bacterial and fungal CEs. Carpet 1 was associated with the highest FBAP concentration in the infant BZ ($2.255\ \text{cm}^{-3}$) but had the fourth lowest loadings of particle mass ($2.79\ \text{g}/\text{m}^2$) and number ($2.28 \times 10^9\ \text{no.}/\text{m}^2$) among the four carpets. Interestingly, while carpet 5 had the highest particle number concentrations in the dust ($2.53 \times 10^{10}\ \#/\text{m}^2$), it had the lowest microbial loading ($4.37 \times 10^8\ \text{CE}/\text{m}^2$). Previous research has demonstrated that carpet type, fiber structure and polymer, usage, and structure of the dust deposit can affect resuspension^{54–56} and biological particle adhesion.⁵⁷ Our results suggest that the magnitude of a person's inhalation

exposure to resuspended *bio*PM can change from carpet to carpet, even within the same home, due to the complexity of the carpet and the *bio*PM which is embedded into it.

Resuspended FBAP concentrations and size distributions generally did not decrease with repeated crawling or walking paths on the same carpet (Figures 3e and S8). In total, each carpet experienced 200 min of crawling and walking across its exposed upward facing surface area. This suggests that resuspension of carpet dust can act as a near-continuous supply of *bio*PM to the BZ over time-scales of several hours, especially if particles have time to redeposit and reaccumulate on the carpet during periods of limited to no human locomotion. While resuspension can lead to significant

elevations in coarse-mode FBAP number and mass concentrations (Figure 3e), the fraction of settled particles that resuspend (resuspension fraction) per physical disturbance is quite small, on the order of 10^{-5} to $10^{-2.7}$. Given the high number concentrations of total particles (10^9 to 10^{10} no./m², >1 μm , Table S1) and bacterial and fungal CEs (10^8 to 10^9 CE/m², Table S1) in the dust, along with high particle deposition loss rates due to gravitational settling (1 to 10 μm : $\sim 1\text{--}3$ h⁻¹, Figure S5), it would take considerable time to deplete the carpet dust *bioPM* reservoir due to resuspension alone.

Respiratory Tract Deposited Dose Rates of Resuspended *bioPM* (FBAPs) in Infant and Adult Respiratory Systems. In 1 min of crawling or walking across a carpet, on the order of 10^3 to 10^4 resuspended FBAPs, with an associated surface area of 10^5 to 10^6 μm^2 , will deposit in the human respiratory system (Figure 4). For an infant, the mean total RTDDR_Fs across five carpets were $6.3 \pm 3.3 \times 10^3$ and $5.7 \pm 2.8 \times 10^3$ deposited FBAPs per minute crawling for nasal and oral breathing, respectively (Figure 4a,e; mean \pm s.d.). The mean total RTDDR_F for an adult was $1.5 \pm 0.72 \times 10^4$ deposited FBAPs per minute walking (Figure 4b), 2.4-fold greater than that of an infant. This difference can be primarily attributed to the adult breathing rate (0.0195 m³ min⁻¹), which is 3.3-fold greater than that of the infant (0.00598 m³ min⁻¹) for light activity. Furthermore, for each minute of walking, approximately 1.6×10^3 FBAPs will deposit in the airways of an adult for every million FBAPs that resuspend (based on emission rate analysis in section S3 and Figure S16: total RTDDR_F/total E_{F_i} ; E_{F_i} s ranged from $\sim 10^8$ to 10^9 FBAPs per hour).

The magnitude of the RTDDR_F for each carpet naturally follows the total FBAP number concentrations shown in Figure 3e, with the greatest RTDDR_Fs found for carpets 1 and 5. Direct comparisons with previous estimates of RTDDR_Fs for *bioPM* are difficult, as they relied on either bulk air measurement of culturable bacteria or fungi, such as ~ 0.1 to 5 CFU/min for indoor culturable fungi by Reponen et al.²⁰ and ~ 6 to 33 CFU/min for culturable bacteria and fungi by Gao et al.,²⁶ or evaluated exposure to fungal spore release directly from an agar plate under high speed jets (1.5×10^3 and 10^4 spores per minute for infants and adults, respectively, by Cho et al.²²). Regarding the latter, the magnitude of RTDDR_Fs reported here are similar as what one would receive inhaling air directly above a moldy material agitated by high air velocities.²²

The tracheobronchial regional RTDDR_F was much greater for infants (41% of total, $2.6 \pm 1.5 \times 10^3$ min⁻¹, nasal) compared to adults (5.4% of total, $8.3 \pm 4.2 \times 10^2$ min⁻¹, nasal; Figures 4a,b and 5). The opposite was true for the head airways, which was the predominant deposition region for adults (84% of total, $1.3 \pm 0.59 \times 10^4$ min⁻¹, nasal). Accounting for hygroscopic growth of inhaled FBAPs resulted in a small increase in the overall total RTDDR_F for both infants and adults but a reduction in the pulmonary regional RTDDR_F by 15% for infants and 13% for adults (Figures 4 and S14). This is consistent with the regional deposition analysis of fungal spores in Reponen et al.⁵⁸

A significant shift in infant respiratory tract deposition patterns can occur if nasal breathing transitions to oral breathing during a crawling period (Figure S6). Upon oral breathing, a reduction in the head airways regional RTDDR_F is associated with both an absolute and relative increase in RTDDR_Fs for the lower airways. For example, on carpet 1, the pulmonary regional RTDDR_F increased from 1.21×10^3 min⁻¹

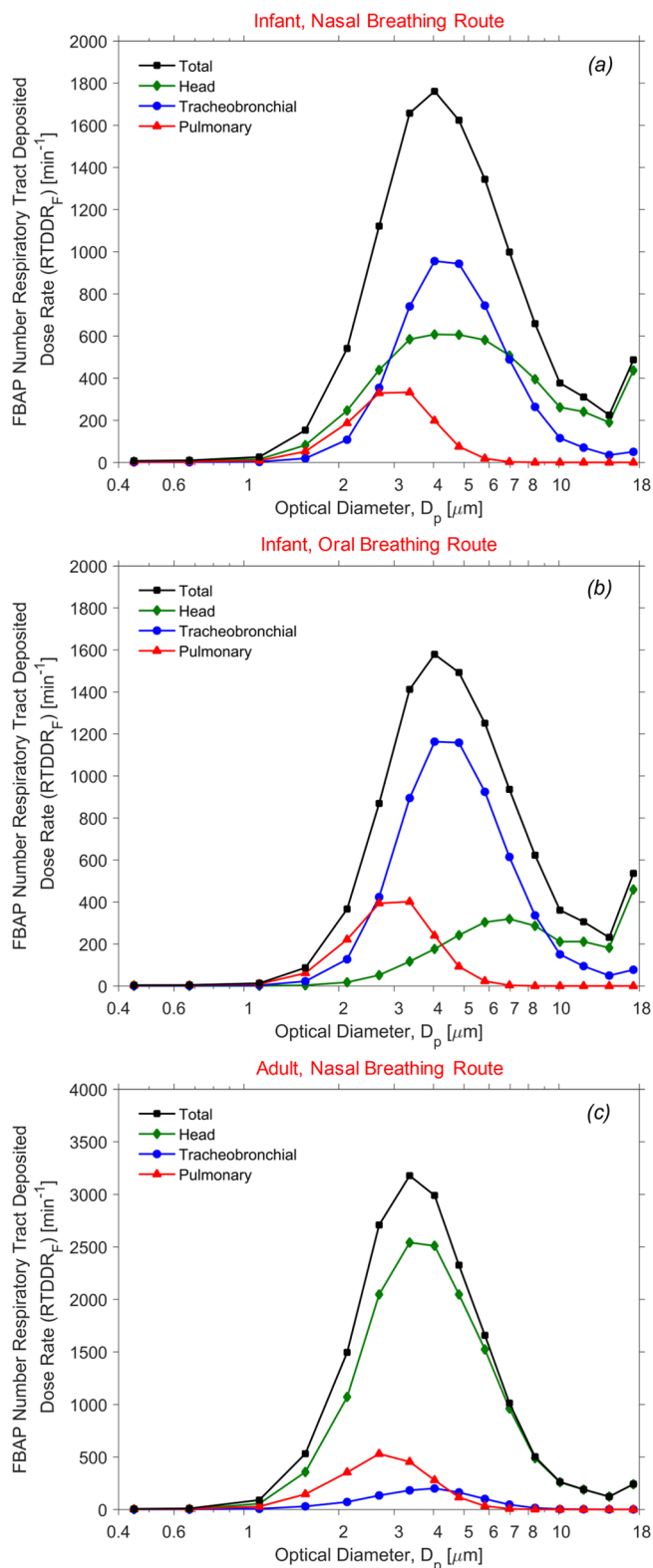


Figure 5. Total and regional size-resolved FBAP number respiratory tract deposited dose rates (RTDDR_Fs; per minute crawling or walking) on carpet 1, for (a) infant crawling, nasal breathing route, (b) infant crawling, oral breathing route, and (c) adult walking, nasal breathing route. Note: a hygroscopic growth factor of 1.12 was applied to the BZ FBAP size distributions, as described in section S2.

for nasal (10.7% of total) to 1.45×10^3 min⁻¹ for oral (14.4% of total) and the tracheobronchial RTDDR_F increased from 4.89

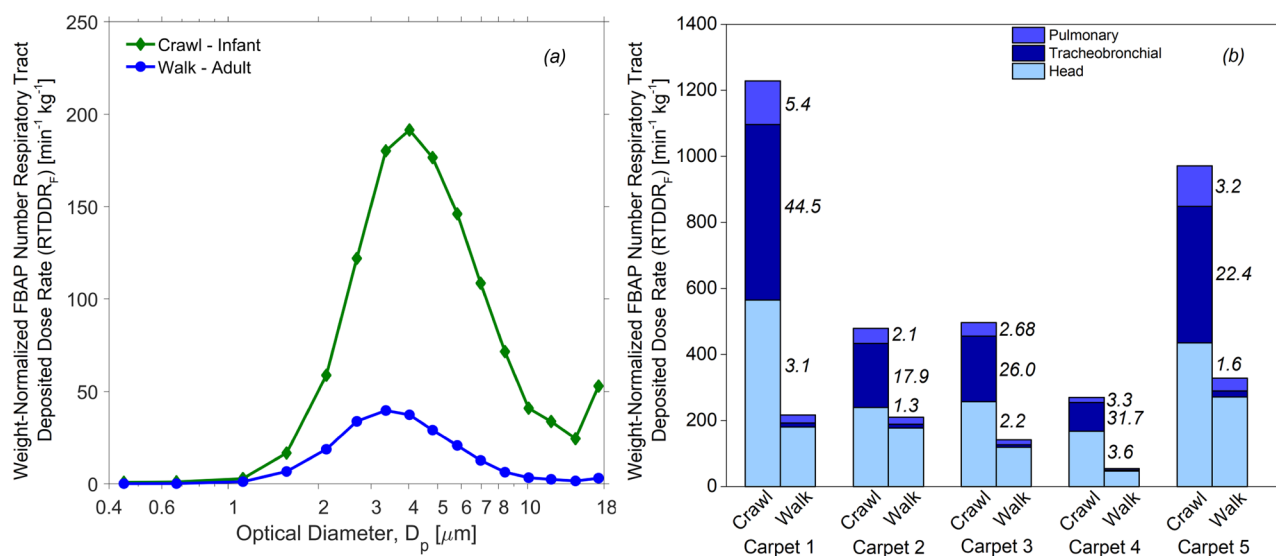


Figure 6. (a) Weight-normalized total size-resolved FBAP number respiratory tract deposited dose rates (RTDDRFs) for infant crawling and adult walking on carpet 1 (both nasal breathing route) and (b) weight-normalized regional size-integrated (0.4–15.4 μm) FBAP number RTDDRFs for infant crawling and adult walking on each of the five carpets (both nasal breathing route). The ratio of the infant to adult weight-normalized FBAP RTDDRF in each region is shown to the right of each infant bar. Note: a hygroscopic growth factor of 1.12 was applied to the BZ FBAP size distributions, as described in section S2.

$\times 10^3 \text{ min}^{-1}$ for nasal (43.3% of total) to $6.04 \times 10^3 \text{ min}^{-1}$ for oral (60% of total). The greater number of resuspended FBAPs that will deposit in the lower respiratory system for oral breathing is important, given the greater prevalence of this breathing route among infants and children compared to adults^{59,60} and the resulting change in potential colonization locations of inhaled bacterial cells and fungal spores.

The size-resolved total RTDDRFs exhibit a prominent mode between 2.5 and 8 μm (Figure 5). For infants, the development of the total RTDDRF mode is the result of the dominant mode of the BZ FBAP size distributions coinciding with the local maxima in depositions fractions for the pulmonary (2–4 μm) and tracheobronchial (3–7 μm) regions, whereas for adults, the mode develops due to the high deposition fractions (>0.7) in the head airways for particles above 3 μm (Figure S6). Thus, for infants, a significant fraction of 3–6 μm agglomerated bacterial cells and fungal spores can penetrate the head airways and deposit and possibly colonize the lower respiratory microbiota. As shown for carpet 1 in Figure 5b, the modal peak in the size-resolved tracheobronchial regional RTDDRF at roughly 4 μm for an infant under oral breathing is approximately $1.15 \times 10^3 \text{ min}^{-1}$, 73% of the corresponding modal peak in the total RTDDRF curve ($1.58 \times 10^3 \text{ min}^{-1}$). Furthermore, the partial second mode in the infant BZ FBAP size distributions above 10 μm (Figures 2 and 3) occurs at the local maxima for deposition fractions in the head airways (Figure S6). Super-10 μm bioPM and abiotic particles will preferentially deposit in this region, with size-resolved head airways regional RTDDRFs for carpet 1 peaking at around $4.3 \times 10^2 \text{ min}^{-1}$ near 18 μm . Lastly, adults will receive much of their dose to 2.5–7 μm bioPM in their upper airways, which can be of concern for those with asthma and allergic rhinitis (e.g.,⁶¹).

Infants inhale considerably more air per kg body mass (650 $\text{cm}^3/\text{kg min}$) than do adults (244 $\text{cm}^3/\text{kg min}$; based on breathing rate data from section S2). This effect was captured through the analysis of weight-normalized RTDDRFs. As shown in Figure 6, an infant receives a 3.88 ± 1.26 -fold greater dose of respiratory tract deposited FBAPs per kg body mass compared

to an adult (mean \pm s.d.). The difference in age-specific weight-normalized RTDDRFs was particularly pronounced in the tracheobronchial region, where they were 22.4- to 44.5-fold greater for an infant compared to an adult. This was also true for FBAPs between 3 and 5 μm (Figure 6a). As suggested in Phalen and Phalen,⁶² weight-normalized RTDDRFs may provide a useful basis to compare the resulting biological effects of exposure to inhaled particles between young children and adults. Alternatively, RTDDRFs can be normalized by lung mass or surface area.⁵⁹ The RTDDRFs reported in this study not only account for infant physiology (respiratory and breathing parameters, body mass) but also a form of human locomotion in belly crawling that is unique to humans under the age of one. The in situ BZ measurement of resuspended FBAPs with a robotic crawling platform allows for a much more accurate determination of early life exposures and RTDDRFs to bioPM than what can be achieved with bulk indoor air sampling (e.g., 1–2 m above infant BZ) or settled house dust analysis.

■ ASSOCIATED CONTENT

📄 Supporting Information

The Supporting Information is available free of charge on the ACS Publications website at DOI: 10.1021/acs.est.7b04183.

Detailed Materials and Methods section along with supplemental results and discussion. (PDF)

Video of the simplified robotic crawling infant used to study how belly crawling resuspends bioPM from carpet dust in a full-scale 80 m^3 experimental chamber. (MP4)

■ AUTHOR INFORMATION

Corresponding Author

*Phone: +1-765-496-0576; e-mail: bboor@purdue.edu.

ORCID

Brandon E. Boor: 0000-0003-1011-4100

Notes

The authors declare no competing financial interest.

ACKNOWLEDGMENTS

We are thankful to the families who donated their carpets to this study. Financial support was provided by Purdue University start-up funds, the U.S. Environmental Protection Agency Science to Achieve Results (STAR) Fellowship Program (Grant No. F13D10740), the U.S. Department of State Fulbright Program, the Centre for International Mobility (CIMO) in Finland, and the American-Scandinavian Foundation. Microbiological work at the National Institute for Health and Welfare was supported by the Academy of Finland (Grant No. 296817). Maria Valkonen is acknowledged for PAMAS particle number analyses for carpet dust.

REFERENCES

- (1) Karlsson, E.; Berglund, T.; Strömqvist, M.; Nordstrand, M.; Fängmark, I. The effect of resuspension caused by human activities on the indoor concentration of biological aerosols. *J. Aerosol Sci.* **1999**, *30*, S737–S738.
- (2) Chen, Q.; Hildemann, L. M. The effects of human activities on exposure to particulate matter and bioaerosols in residential homes. *Environ. Sci. Technol.* **2009**, *43* (13), 4641–4646.
- (3) Raja, S.; Xu, Y.; Ferro, A. R.; Jaques, P. A.; Hopke, P. K. Resuspension of indoor aeroallergens and relationship to lung inflammation in asthmatic children. *Environ. Int.* **2010**, *36* (1), 8–14.
- (4) Goebes, M. D.; Boehm, A. B.; Hildemann, L. M. Contributions of foot traffic and outdoor concentrations to indoor airborne *Aspergillus*. *Aerosol Sci. Technol.* **2011**, *45* (3), 352–363.
- (5) Hospodsky, D.; Qian, J.; Nazaroff, W. W.; Yamamoto, N.; Bibby, K.; Rismani-Yazdi, H.; Peccia, J. Human occupancy as a source of indoor airborne bacteria. *PLoS One* **2012**, *7* (4), e34867.
- (6) Adams, R. I.; Bhangar, S.; Pasut, W.; Arens, E. A.; Taylor, J. W.; Lindow, S. E.; Nazaroff, W. W.; Bruns, T. D. Chamber bioaerosol study: Outdoor air and human occupants as sources of indoor airborne microbes. *PLoS One* **2015**, *10* (5), e0128022.
- (7) Qian, J.; Peccia, J.; Ferro, A. R. Walking-induced particle resuspension in indoor environments. *Atmos. Environ.* **2014**, *89*, 464–481.
- (8) Boor, B. E.; Spilak, M. P.; Corsi, R. L.; Novoselac, A. Characterizing particle resuspension from mattresses: chamber study. *Indoor Air* **2015**, *25* (4), 441–456.
- (9) Adolph, K. Motor and physical development: Locomotion. In *Encyclopedia of infant and early childhood development*; Academic Press: New York, 2008.
- (10) Shalat, S. L.; Stambler, A. A.; Wang, Z.; Mainelis, G.; Emoekpere, O. H.; Hernandez, M.; Liroy, P. J.; Black, K. Development and in-home testing of the pretoddler inhalable particulate environmental robotic (PIPER Mk IV) sampler. *Environ. Sci. Technol.* **2011**, *45* (7), 2945–2950.
- (11) Wang, Z.; Shalat, S. L.; Black, K.; Liroy, P. J.; Stambler, A. A.; Emoekpere, O. H.; Hernandez, M.; Han, T.; Ramagopal, M.; Mainelis, G. Use of a robotic sampling platform to assess young children's exposure to indoor bioaerosols. *Indoor Air* **2012**, *22* (2), 159–169.
- (12) Sagona, J. A.; Shalat, S. L.; Wang, Z.; Ramagopal, M.; Black, K.; Hernandez, M.; Mainelis, G. Evaluation of particle resuspension in young children's breathing zone using stationary and robotic (PIPER) aerosol samplers. *J. Aerosol Sci.* **2015**, *85*, 30–41.
- (13) Nazaroff, W. W. Indoor bioaerosol dynamics. *Indoor Air* **2016**, *26* (1), 61–78.
- (14) Huffman, J. A.; Treutlein, B.; Pöschl, U. Fluorescent biological aerosol particle concentrations and size distributions measured with an ultraviolet aerodynamic particle sizer (UV-APS) in Central Europe. *Atmos. Chem. Phys.* **2009**, *9* (4), 17705–17751.
- (15) Gabey, A. M.; Gallagher, M. W.; Whitehead, J.; Dorsey, J. R.; Kaye, P. H.; Stanley, W. R. Measurements and comparison of primary biological aerosol above and below a tropical forest canopy using a dual channel fluorescence spectrometer. *Atmos. Chem. Phys.* **2010**, *10* (10), 4453–4466.
- (16) Pöhlker, C.; Huffman, J. A.; Pöschl, U. Autofluorescence of atmospheric bioaerosols - Fluorescent biomolecules and potential interferences. *Atmos. Meas. Tech.* **2012**, *5* (1), 37–71.
- (17) Saari, S. E.; Reponen, T.; Keskinen, J. Performance of Two Fluorescence-Based Real-Time Bioaerosol Detectors: BioScout vs. UVAPS. *Aerosol Sci. Technol.* **2014**, *48* (4), 371–378.
- (18) Saari, S. E.; Putkiranta, M. J.; Keskinen, J. Fluorescence spectroscopy of atmospherically relevant bacterial and fungal spores and potential interferences. *Atmos. Environ.* **2013**, *71*, 202–209.
- (19) Hewett, P. Limitations in the use of particle size-selective sampling criteria in occupational epidemiology. *Appl. Occup. Environ. Hyg.* **1991**, *6* (4), 290–300.
- (20) Reponen, T. Aerodynamic diameters and respiratory deposition estimates of viable fungal particles in mold problem dwellings. *Aerosol Sci. Technol.* **1995**, *22* (1), 11–23.
- (21) Venkataraman, C. Comparison of particle lung doses from the fine and coarse fractions of urban PM-10 aerosols. *Inhalation Toxicol.* **1999**, *11* (2), 151–169.
- (22) Cho, S.-H.; Seo, S.-C.; Schmechel, D.; Grinshpun, S. A.; Reponen, T. Aerodynamic characteristics and respiratory deposition of fungal fragments. *Atmos. Environ.* **2005**, *39* (30), 5454–5465.
- (23) Löndahl, J.; Massling, A.; Pagels, J.; Swietlicki, E.; Vaclavik, E.; Loft, S. Size-resolved respiratory-tract deposition of fine and ultrafine hydrophobic and hygroscopic aerosol particles during rest and exercise. *Inhalation Toxicol.* **2007**, *19* (2), 109–116.
- (24) Koivisto, A. J.; Aromaa, M.; Mäkelä, J. M.; Pasanen, P.; Hussein, T.; Hämeri, K. Concept to estimate regional inhalation dose of industrially synthesized nanoparticles. *ACS Nano* **2012**, *6* (2), 1195–1203.
- (25) Hussein, T.; Löndahl, J.; Paasonen, P.; Koivisto, A. J.; Petäjä, T.; Hämeri, K.; Kulmala, M. Modeling regional deposited dose of submicron aerosol particles. *Sci. Total Environ.* **2013**, *458*, 140–149.
- (26) Gao, M.; Jia, R.; Qiu, T.; Han, M.; Song, Y.; Wang, X. Seasonal size distribution of airborne culturable bacteria and fungi and preliminary estimation of their deposition in human lungs during non-haze and haze days. *Atmos. Environ.* **2015**, *118*, 203–210.
- (27) Manigrasso, M.; Buonanno, G.; Fuoco, F. C.; Stabile, L.; Avino, P. Aerosol deposition doses in the human respiratory tree of electronic cigarette smokers. *Environ. Pollut.* **2015**, *196*, 257–267.
- (28) Hubal, E. A. C.; Sheldon, L. S.; Burke, J. M.; McCurdy, T. R.; Berry, M. R.; Rigas, M. L.; Zartarian, V. G.; Freeman, N. C. Children's exposure assessment: a review of factors influencing children's exposure, and the data available to characterize and assess that exposure. *Environ. Health Perspect.* **2000**, *108* (6), 475.
- (29) Saari, S. E.; Mensah-Attipoe, J.; Reponen, T.; Veijalainen, A. M.; Salmela, A.; Pasanen, P.; Keskinen, J. Effects of fungal species, cultivation time, growth substrate, and air exposure velocity on the fluorescence properties of airborne fungal spores. *Indoor Air* **2015**, *25* (6), 653–661.
- (30) Saari, S. E.; Niemi, J.; Rönkkö, T.; Kuuluvainen, H.; Järvinen, A.; Pirjola, L.; Aurela, M.; Hillamo, R.; Keskinen, J. Seasonal and diurnal variations of fluorescent bioaerosol concentration and size distribution in the urban environment. *Aerosol Air Qual. Res.* **2015**, 572–581.
- (31) Hyytiäinen, H.; Jayaprakash, B.; Kirjavainen, P.; Saari, S.; Holopainen, R.; Keskinen, J.; Hämeri, K.; Hyvärinen, A.; Boor, B. E.; Täubel, M. Crawling-Induced floor dust resuspension affects the microbiota of the infant breathing zone. *Microbiome*, In Press.
- (32) Kretch, K. S.; Franchak, J. M.; Adolph, K. E. Crawling and walking infants see the world differently. *Child Dev.* **2014**, *85* (4), 1503–1518.
- (33) Bhangar, S.; Huffman, J. A.; Nazaroff, W. W. Size-resolved fluorescent biological aerosol particle concentrations and occupant emissions in a university classroom. *Indoor Air* **2014**, *24*, 604–617.
- (34) Toprak, E.; Schnaiter, M. Fluorescent biological aerosol particles measured with the Waveband Integrated Bioaerosol Sensor WIBS-4: Laboratory tests combined with a one year field study. *Atmos. Chem. Phys.* **2013**, *13* (1), 225–243.
- (35) Valsan, A. E.; Ravikrishna, R.; Biju, C. V.; Pöhlker, C.; Després, V. R.; Huffman, J. A.; Pöschl, U.; Gunthe, S. S. Fluorescent biological

aerosol particle measurements at a tropical high-altitude site in southern India during the southwest monsoon season. *Atmos. Chem. Phys.* **2016**, *16* (15), 9805–9830.

(36) Després, V. R.; Huffman, J. A.; Burrows, S. M.; Hoose, C.; Safatov, A. S.; Buryak, G.; Fröhlich-Nowoisky, J.; Elbert, W.; Andreae, M. O.; Pöschl, U.; Jaenicke, R. Primary biological aerosol particles in the atmosphere: A review. *Tellus, Ser. B* **2012**, *64* (1), 15598.

(37) Hernandez, M.; Perring, A. E.; McCabe, K.; Kok, G.; Granger, G.; Baumgardner, D. Chamber catalogues of optical and fluorescent signatures distinguish bioaerosol classes. *Atmos. Meas. Tech.* **2016**, *9* (7), 3283–3292.

(38) Davies, R. R.; Noble, W. C. Dispersal of bacteria on desquamated skin. *Lancet* **1962**, *280* (7269), 1295–1297.

(39) Noble, W. C.; Davies, R. R.; Place, D. A. Studies on the dispersal of staphylococci. *J. Clin. Pathol.* **1965**, *18* (1), 16–19.

(40) Lighthart, B. Mini-review of the concentration variations found in the alfresco atmospheric bacterial populations. *Aerobiologia (Bologna)* **2000**, *16* (1), 7–16.

(41) Gorny, R. L.; Dutkiewicz, J.; Krysinska-Traczyk, E. Size distribution of bacterial and fungi bioaerosols in indoor air. *Ann. Agric. Environ. Med.* **1999**, *6*, 105–113.

(42) Huffman, J. A.; Sinha, B.; Garland, R. M.; Snee-Pollmann, A.; Gunthe, S. S.; Artaxo, P.; Martin, S. T.; Andreae, M. O.; Pöschl, U. Size distributions and temporal variations of biological aerosol particles in the Amazon rainforest characterized by microscopy and real-time UV-APS fluorescence techniques during AMAZE-08. *Atmos. Chem. Phys.* **2012**, *12* (24), 11997–12019.

(43) Qian, J.; Hospodsky, D.; Yamamoto, N.; Nazaroff, W. W.; Peccia, J. Size-resolved emission rates of airborne bacteria and fungi in an occupied classroom. *Indoor Air* **2012**, *22* (4), 339–351.

(44) Hospodsky, D.; Yamamoto, N.; Nazaroff, W. W.; Miller, D.; Gorthala, S.; Peccia, J. Characterizing airborne fungal and bacterial concentrations and emission rates in six occupied children's classrooms. *Indoor Air* **2015**, *25* (6), 641–652.

(45) Reponen, T.; Grinshpun, S. A.; Conwell, K. L.; Wiest, J.; Anderson, M. Aerodynamic versus physical size of spores: measurement and implication for respiratory deposition. *Grana* **2001**, *40* (3), 119–125.

(46) Kanaani, H.; Hargreaves, M.; Smith, J.; Ristovski, Z.; Agranovski, V.; Morawska, L. Performance of UVAPS with respect to detection of airborne fungi. *J. Aerosol Sci.* **2008**, *39* (2), 175–189.

(47) Hussein, T.; Norros, V.; Hakala, J.; Petäjä, T.; Aalto, P. P.; Rannik, Ü.; Vesala, T.; Ovaskainen, O. Species traits and inertial deposition of fungal spores. *J. Aerosol Sci.* **2013**, *61*, 81–98.

(48) Mackintosh, C. A.; Lidwell, O. M.; Towers, A. G.; Marples, R. R. The dimensions of skin fragments dispersed into the air during activity. *J. Hyg.* **1978**, *81* (3), 471–480.

(49) Custovic, A.; Woodcock, H.; Craven, M.; Hassall, R.; Hadley, E.; Simpson, A.; Woodcock, A. Dust mite allergens are carried on not only large particles. *Pediatr. Allergy Immunol.* **1999**, *10* (4), 258–260.

(50) Montoya, L. D.; Hildemann, L. M. Size distributions and height variations of airborne particulate matter and cat allergen indoors immediately following dust-disturbing activities. *J. Aerosol Sci.* **2005**, *36* (5–6), 735–749.

(51) Pereira, M. L.; Knibbs, L. D.; He, C.; Grzybowski, P.; Johnson, G. R.; Huffman, J. A.; Bell, S. C.; Wainwright, C. E.; Matte, D. L.; Dominski, F. H.; et al. Sources and dynamics of fluorescent particles in hospitals. *Indoor Air* **2017**, *27* (5), 988–1000.

(52) Gorny, R. L.; Reponen, T.; Willeke, K.; Schmechel, D.; Robine, E.; Boissier, M.; Grinshpun, S. A. Fungal fragments as indoor air biocontaminants. *Appl. Environ. Microbiol.* **2002**, *68* (7), 3522–3531.

(53) Pazmandi, K.; Kumar, B. V.; Szabo, K.; Boldogh, I.; Szoor, A.; Vereb, G.; Veres, A.; Lanyi, A.; Rajnavolgyi, E.; Bacsi, A. Ragweed subpollen particles of respirable size activate human dendritic cells. *PLoS One* **2012**, *7* (12), e52085.

(54) Tian, Y.; Sul, K.; Qian, J.; Mondal, S.; Ferro, A. R. A comparative study of walking-induced dust resuspension using a consistent test mechanism. *Indoor Air* **2014**, *24* (6), 592–603.

(55) Rosati, J. A.; Thornburg, J.; Rodes, C. Resuspension of particulate matter from carpet due to human activity. *Aerosol Sci. Technol.* **2008**, *42* (6), 472–482.

(56) Boor, B. E.; Siegel, J. A.; Novoselac, A. Monolayer and multilayer particle deposits on hard surfaces: literature review and implications for particle resuspension in the indoor environment. *Aerosol Sci. Technol.* **2013**, *47* (8), 831–847.

(57) Thio, B. J. R. *Characterization of bioparticulate adhesion to synthetic carpet polymers with atomic force microscopy*; Georgia Institute of Technology: Atlanta, GA, 2009.

(58) Reponen, T.; Willeke, K.; Ulevicius, V.; Reponen, A.; Grinshpun, S. A. Effect of relative humidity on the aerodynamic diameter and respiratory deposition of fungal spores. *Atmos. Environ.* **1996**, *30* (23), 3967–3974.

(59) Foos, B.; Marty, M.; Schwartz, J.; Bennett, W.; Moya, J.; Jarabek, A. M.; Salmon, A. G. Focusing on children's inhalation dosimetry and health effects for risk assessment: an introduction. *J. Toxicol. Environ. Health, Part A* **2007**, *71* (3), 149–165.

(60) Bennett, W. D.; Zeman, K. L.; Jarabek, A. M. Nasal contribution to breathing and fine particle deposition in children versus adults. *J. Toxicol. Environ. Health, Part A* **2007**, *71* (3), 227–237.

(61) Baldacci, S.; Maio, S.; Cerrai, S.; Sarno, G.; Baiz, N.; Simoni, M.; Annesi-Maesano, I.; Viegi, G. Allergy and asthma: Effects of the exposure to particulate matter and biological allergens. *Respir. Med.* **2015**, *109* (9), 1089–1104.

(62) Phalen, R. F.; Phalen, R. N. *Introduction to air pollution science*; Jones & Bartlett Publishers: Burlington, MA, 2012.

■ NOTE ADDED AFTER ASAP PUBLICATION

There was an error in the unit of the highest FBAP concentration in the infant BZ of the version of this article published November 29, 2017. The unit was corrected and reposted on December 5, 2017.